Firstly, we would like to thank both editor and referees for their important comments, and we have revised our manuscript accordingly. The original comments from referees are in black, our replies are in blue and the changes in original manuscript are in red.

We thank the Editor for reconsidering our manuscript. Before addressing the individual comments, we would like to clarify that our analysis focuses on aerosol characteristics associated with regionally transported air masses reaching this remote site during daytime conditions. In our previous response, we have clarified that our analysis was conducted within defined air mass dominated periods identified based on transport origin. Within each of these periods, the air masses exhibited relatively consistent characteristics in terms of source region and meteorological conditions. We addressed the reviewers' concerns by incorporating an above-canopy analysis, which demonstrates that the boundary layer was well mixed during the daytime throughout the campaign period. The influence of localized emissions and nearby plumes during daytime is minimal and does not compromise the conclusions of this study. To reduce the ambiguity on this respect, we have revised the description of the experiment in the Introduction, as presented later in our response.

Following the editor's suggestion, in this revision, we further calculated air mass transport age using back trajectories calculated with the UK Met Office NAME dispersion model to provide an independent validation of the temporal variability of the relative anthropogenic photochemical age ($t_{\mathrm{anthrop-photo}}$) inferred from NO_x/NO_y ratios, which are based on the assumption that air masses with longer transport times generally experience longer cumulative photochemical processing. In the trajectory-based analysis, the dominant anthropogenic emission regions associated with each air mass cluster was identified using the EDGAR regional emission inventory corresponding to the campaign period. The trajectory-based transport age was then estimated as the earliest backward-trajectory time at which the air mass entered its corresponding dominant anthropogenic emission region.

If local NO_x emissions had substantially influenced the NO_x/NO_y-based photochemical age, a pronounced divergence of temporal trends from the trajectory-derived transport age would be expected because trajectory-derived transport age does not account for local pollution influences from Paris region. However, according to our results, the temporal variation of the air mass transport age estimated from the dispersion model shows good agreement with $t_{\mathrm{anthrop-photo}}$ derived from the NO_x/NO_y ratio during daytime (06:00–20:00 local time) as shown below in panel a of Fig. 3 and Fig. S13, although their absolute values differ due to the distinct estimation approaches. This consistency indicates that the NO_x/NO_y-based photochemical age used in this study provides a robust representation of the relative aging of transported air masses and the impact of local emissions on the NO_x/NO_y-based $t_{\mathrm{anthrop-photo}}$ estimates was minimal. This agreement suggests that the temporal variability in NO_x/NO_y was primarily governed by cumulative transport and photochemical processing, rather than being dominated by intermittent local NO_x injections from Paris.

Because the NO_x/NO_y-derived $t_{anthrop-photo}$ provides higher temporal resolution than the trajectory-based transport age, we retain $t_{anthrop-photo}$ in our analysis, whereas the trajectory-based transport age was used for independent validation. We have revised the back dispersion model section to include a description of the method used to estimate the trajectory-based transport age:

Accordingly, the following text in red was added in the main text of the manuscript in Section 2.6.2 (Page 8 – Page 9, L248 – L264):

2.6.2 Estimation of trajectory-based plume transport age

Plume transport age was derived from backward air-mass trajectories to provide an independent validation of $t_{anthrop-photo}$ inferred from NO_x/NO_y ratios. Backward air-mass trajectories were simulated using the NAME model with the same model domain as applied in the backward dispersion analysis. The model generated 24-h backward trajectories by releasing ensembles of Lagrangian particles at hourly intervals and tracking their transport on a 0.25° × 0.25° grid, with particle positions recorded every 15 min. For each backward trajectory, the dominant potential air-mass source region was first identified following the method described in Sect. 2.6.1. The EDGAR anthropogenic $PM_{2.5}$ emission inventory (0.01° × 0.01° resolution, reported as total $PM_{2.5}$ emission in Tg) (Crippa et al., 2024) for the campaign period (June–July 2022) was used to determine the dominant anthropogenic emission areas associated with each identified source region (Figure S12). The emission inventory indicates that no major anthropogenic emission hotspots are present between these source regions and the measurement site, supporting the interpretation that the observed air masses reflect regional-scale transport without substantial intermediate source contributions. The plume transport age was defined as the time elapsed between the observation time at the measurement site and the first backward-trajectory intersection with the corresponding anthropogenic emission region. The trajectory-derived transport age serves as a relative indicator for validating the temporal variability of $t_{anthrop-photo}$ based on the assumption that air masses with longer transport times generally experience longer cumulative photochemical processing. Detailed comparison between $t_{anthrop-photo}$ and transport age is presented in Section S10 in the supplementary.

The diurnal mean transport age has been added to Figure 3:

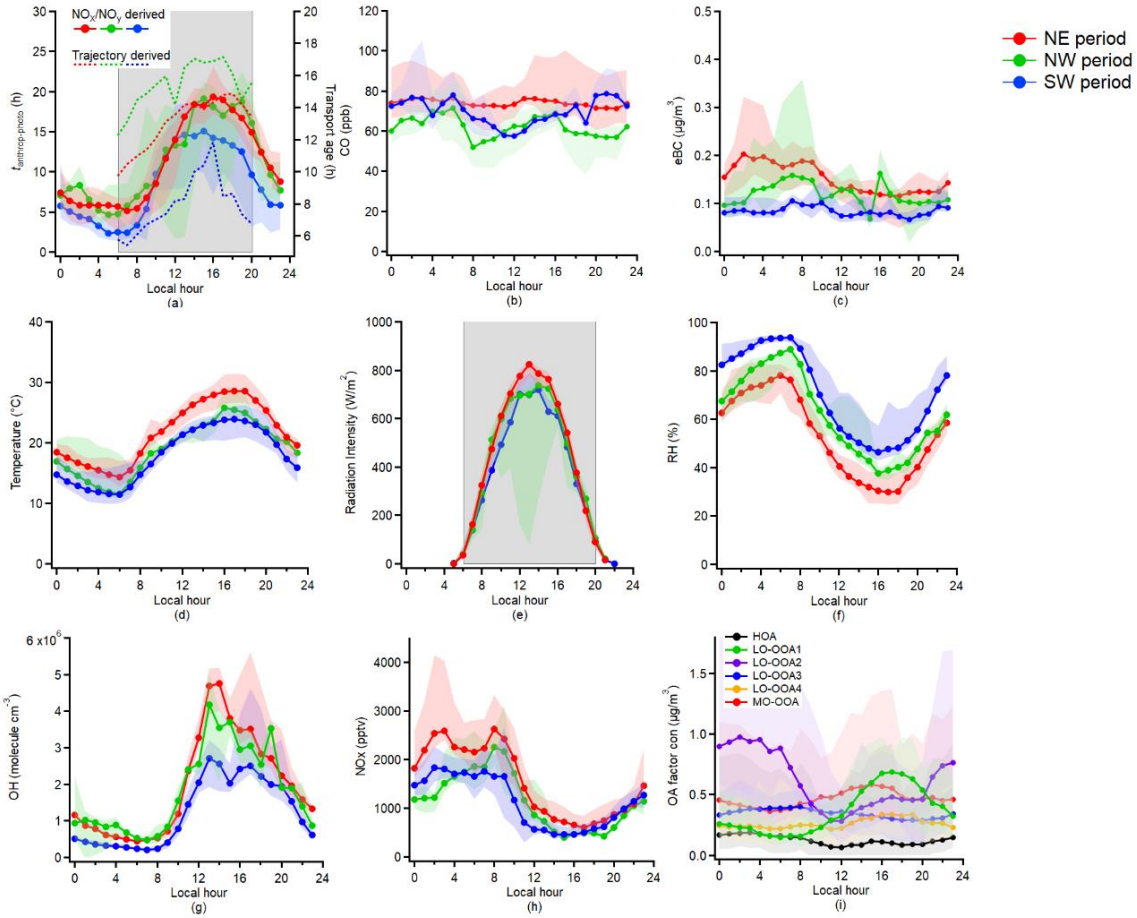

Figure 3: Diurnal variation of the (a) Relative anthropogenic photochemical age ($t_{\mathrm{anthrop-photo}}$) derived from NO_x/NO_y ratio and trajectory-derived transport age; (b) CO mixing ratio; (c) eBC mass concentration; (d) Temperature; (e) Radiation Intensity; (f) RH; (g) OH concentration; (h) NO_x concentration; (i) PMF OA factors. The grey shades in (a) and (e) indicate the periods for the photochemical aging analysis. The lower and upper whiskers in the figure are the 25th and 75th percentiles, respectively.

The description of Figure 3 in Section 3.1 (Page 10, L289 – L294) has been updated:

As shown in Figure 3(a), the diurnal variation of $t_{\mathrm{anthrop-photo}}$ followed that of the trajectory-based transport age derived from the NAME dispersion model. As presented in Section S10 of the supplementary, these two independent indicators exhibited comparable temporal trends, supporting the use of $t_{\mathrm{anthrop-photo}}$ as a proxy for relative photochemical aging during the campaign. In addition, as illustrated in Figures 3(a) and 3(g), the diurnal pattern of $t_{\mathrm{anthrop-photo}}$ was consistent with the observed diurnal cycles of OH concentration and radiation intensity, further supporting its robustness as a relative indicator of photochemical aging.

The information regarding the emission area and the comparison between NO_x/NO_y -based photochemical age and trajectory-based transport age has been added to the SI as Section S10 (Page 11 – Page 13, L114 – L141):

S10 Evaluation of NO_x/NO_y-derived relative anthropogenic photochemical age

To validate whether NO_x/NO_y-derived $t_{\mathrm{anthrop-photo}}$ provides a robust representation of the relative aging of transported air masses, a trajectory-based transport age was derived as an independent validation. The trajectory-based transport age is defined as the time elapsed between the observation time at the measurement site and the first intersection of the backward trajectory with the corresponding anthropogenic emission region. The trajectory-based transport age was calculated from hourly NAME model outputs.

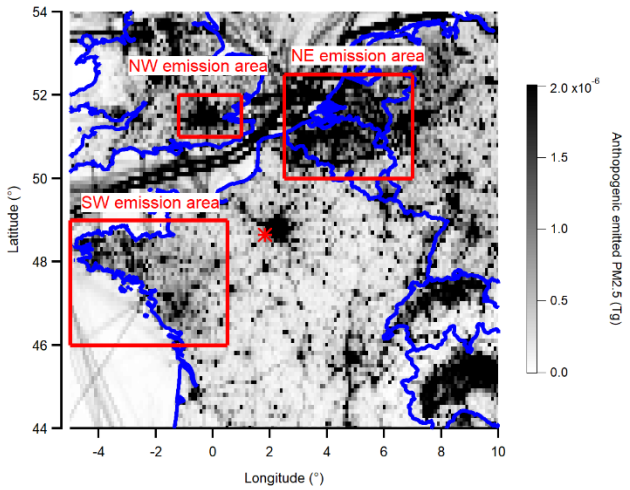

Figure S12. Spatial distribution of anthropogenic $PM_{2.5}$ emissions from the EDGAR inventory, averaged over June–July 2022. Three anthropogenic emission regions were identified based on high-emission hotspots.

As presented in Figure S12, three dominant anthropogenic emission areas were identified through the EDGAR anthropogenic $PM_{2.5}$ emission inventory during the campaign period: (1) NE emission region, (50° – 52.5° N, 2.5° – 7° E); (2) NW emission region (51° – 52°N, -1.2° – 1°E); (3) SW region (46° – 49° N, -5° – 0.5° E). As shown in Figure 2, the SE air mass influenced the site only for a few hours during the afternoon of 19 July. Therefore, emissions from the Po Valley in the SE region were not considered here.

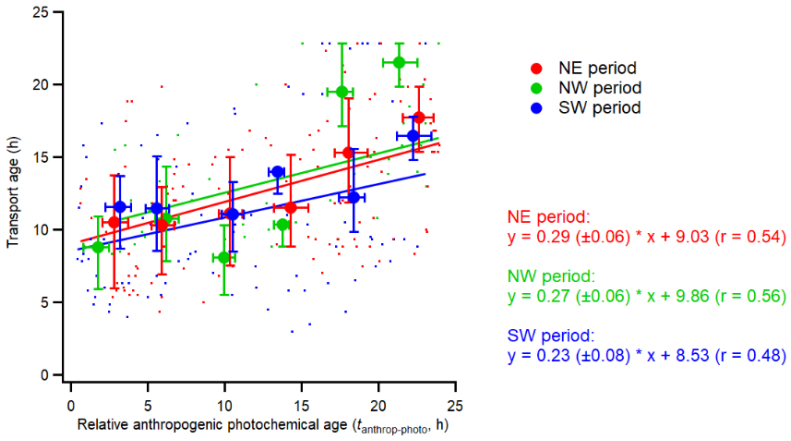

Figure S13 Comparison of the temporal trends in trajectory-based transport age and $t_{\mathrm{anthrop-photo}}$ derived

from NO_x/NO_y ratios. The large markers represent the 4-hour binned averages, and the lower and upper whiskers indicate the 25th and 75th percentiles, respectively. The linear regression was performed using all data points within the same air-mass dominated period, and the fitting uncertainty represents ±1 standard deviation of the fit.

Figure S13 compares the trajectory-based transport age with $t_{\mathrm{anthrop-photo}}$ derived from NO_x/NO_y ratios for different air mass-dominated periods. If local NO_x emissions had substantially influenced the NO_x/NO_y-based $t_{\mathrm{anthrop-photo}}$, a pronounced divergence of temporal trends from the trajectory-based transport age would be expected because the trajectory-based transport age does not account for local pollution influences from Paris region. However, according to our results, the temporal evolution of $t_{\mathrm{anthrop-photo}}$ showed consistent temporal trends with those of the transport age, with moderate correlations (r = 0.48–0.56) across the different periods, suggesting that the impact of local emissions on the NO_x/NO_y-based $t_{\mathrm{anthrop-photo}}$ estimates was minimal. While the correlations were moderate, this level of agreement is expected given the fundamentally different estimation approaches. Trajectory-based transport age reflects the elapsed time associated with regional transport only and thus is characterised by systematically larger baseline values. Nevertheless, the comparable temporal trends between these independent indicators support the use of $t_{\mathrm{anthrop-photo}}$ as a proxy for relative photochemical aging during the campaign, as air masses with longer transport times generally undergo more extensive cumulative photochemical processing.

In addition, we believe this misunderstanding arose from the way the experiment was described in the Introduction. The relevant description in the Introduction section (Page 3, L80-98) has now been revised accordingly:

Paris is one of the most developed and densely populated megacities in Europe, facing significant air pollution challenges. In the past decades, extensive research has been conducted to identify and characterize the properties of particulate pollutants in the Paris region (e.g. (Beekmann et al., 2015)). Previous aerosol mass spectrometer studies (Stirnberg et al., 2021; Bressi et al., 2013; Petit et al., 2015; Healy et al., 2013) indicate that Paris is often affected by the mid-range to long-range transport pollutants attribute to the flat orography of the city. Previous AMS-PMF analysis during summertime have shown that, in addition to the significant contributions from the continental polluted air mass to the total particulate matter with aerodynamic diameter less than 1 μm (PM_1), Paris peri-urban area is also influenced by emissions from the Atlantic Ocean (Crippa et al., 2013). Previous investigations (Healy et al., 2013; Crippa et al., 2013; Petit et al., 2015) in the Paris region were primarily carried out in urban and peri-urban environments, where strong local anthropogenic emissions may obscure regional transport signals and introduce biases in characterising aerosol aging processes. However, most of these studies were conducted more than a decade ago. In recent years, ozone (O_3) has emerged as a major pollutant in European urban areas, and reductions in nitrogen oxides (NO_x) have been reported to contribute to increasing urban O_3 concentrations (Grange et al., 2021). These changes imply a shift in atmospheric oxidation capacity, highlighting the need to reassess the evolution of aerosol

physicochemical properties during transport under present-day chemical regimes. To address these issues, the Atmospheric Chemistry of the Suburban Forest (ACROSS) project (Cantrell and Michoud, 2022) included a ground-based field campaign included a ground-based field campaign in a forested suburban site to capture regionally transported air masses arriving in the Paris region. In this study, we analyse those observations to examine the evolution of aerosol chemical composition in relation to photochemical processing, with particular emphasis on its implications for aerosol optical properties in ambient conditions.

Editor's comments

Thank you for having submitted your revised manuscript. I have reviewed your revisions, responses to the reviewers, and their additional assessment. Considering all the concerns raised, I cannot accept your manuscript for publication. I agree with the 2nd reviewer's comment that photochemical age calculations based on NOx/NOy does not work when anthropogenic and biogenic air masses are mixed in, which is the case at your sampling site. This underlines a lot of your analysis (e.g., as you try to investigate the evolution of different OA factors with age). If you are willing to use another approach to investigate air mass history and aging (e.g., transport time form the model?) and provide major revisions to address this deficiency, I am happy to consider the paper again. If you decide to resubmit with major revisions, please also address the remaining comments from both reviewers and my additional questions and concerns listed below.

I appreciate your effort in submitting your best work.
Roya Bahreini

We thank the editor for reviewing our manuscript and the previous revision. Following the editor's suggestion, we have estimated the air mass transport age using the dispersion model results to provide an independent validation of the temporal variability of the relative anthropogenic photochemical age. The added transport age results are described in detail in our earlier response.

- It's unclear to me why the SE sector has not been considered the same way in the analysis despite a large contribution to air masses sampled in the beginning and end of the campaign.

We appreciate the editor's query. As shown in Figure 2, the influence of the SE air mass (marked in purple) affected the site significantly only for a few hours during the afternoon of 19 July. Because the SE air mass influenced the site for only a very limited period, it was not included in the subsequent analysis. In addition, the SE air mass–dominated period coincided with the biomass-burning-influenced period, however, a distinct biomass burning organic aerosol (BBOA) factor was not identified in the AMS analysis; therefore, this period was excluded from further analysis.

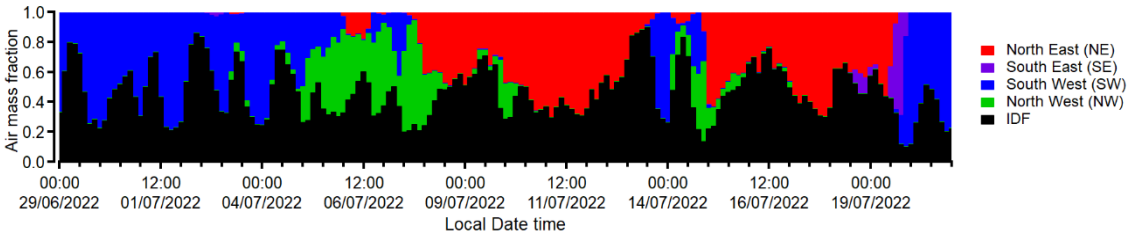

- L272: clarify as "a relative photochemical indicator". Also in L360, change "absolute" to "relative anthropogenic photochemical age"

How does correlation of LO-OOA1 look against isoprene+MVK+MACR?

We have revised the phrasing of the term "relative" to improve clarity. Revied L272 is presented in our response earlier. Following Reviewer #2's comments, we revised the analysis to use absolute concentrations. As the exponential fit was no longer sufficiently robust, it has been removed, and the related text (including L360) has been revised accordingly.

The correlation between LO-OOA1 and (isoprene + MVK + MACR) was r = 0.45, which was comparable to the correlations observed with isoprene (r = 0.43) and MVK+MACR (r = 0.45) individually. We have revised the description in Section 3.2 (Page 9 – Page 10, L279 – L283):

The correlation analysis indicates that they were associated with secondary formation from a mixture of biogenic precursors: while LO-OOA1 exhibited fair correlation with isoprene (r = 0.43), the sum of methyl vinyl ketone (MVK) and methacrolein (MACR) (r = 0.45) and the sum of isoprene, MVK, and MACR (r = 0.45), LO-OOA2 correlated more strongly with monoterpene (r = 0.79).

- LO-OOA2 is suggested to be related to SOA formation from monoterpenes. However, the correlation with toluene is also relatively good. Please comment.

We appreciate the editor's comments. We acknowledge that this feature may arise from two reasons: 1) measurement uncertainties associated with the unit mass resolution of the PTR-MS; In particular, a fraction of monoterpenes is known to fragment under PTR-MS ionization conditions, producing ions at m/z 93 ($C_7H_9^+$) that overlap with the primary ion signal of toluene. As a result, part of the signal attributed to toluene may include contributions from fragmentation of monoterpenes (Tani et al., 2003) and biogenic compound related to monoterpenes (such as p-cymene, (Ambrose et al., 2010)), leading to a potential positive bias in the reported toluene concentrations. This issue can be pronounced at this remote measurement site with low toluene concentrations. 2) Some of the vegetations may also contribute to the emission of toluene as indicated in previous studies (Misztal et al., 2015) and confirmed by diurnal profile of toluene measured by online GC-FID free from monoterpene interference at the site. These two reasons also led to the limited variability in the reported (Toluene + Benzene)/CO concentrations, as noted later in our response to the editor's comment. We have added the discussions in Section 3.2 (Page 11, L332 – L340)

The correlation between LO-OOA2 and toluene (r = 0.73) may be due to two reasons. Firstly, it may arise from instrumental interference, as a fraction of monoterpenes is known to fragment under PTR-MS ionization conditions and produce ions at m/z 93 ($C_7H_9^+$) (Tani et al., 2003; Ambrose et al., 2010), which overlap with the ion signal of toluene. This effect was particularly pronounced at this remote measurement site, where ambient toluene concentrations were low. Secondly, toluene may also originate from biogenic sources. Previous studies (Misztal et al., 2015; White et al., 2009) have shown that certain vegetation types can also emit toluene, indicating that not all observed toluene necessarily derives from anthropogenic emissions. Given these two reasons, toluene may not serve as a reliable tracer of anthropogenic primary sources, as only limited temporal variability relative to CO was observed during the campaign (presented in Section S7 in the supplementary).

- L322: The statement that marine aerosol only in the form of sea salt impacted the site and not MSA-driven organics doesn't make sense.

We appreciate the Editor's concern. However, a detailed source attribution of this PMF-derived OOA factor (LO-OOA3) is not warranted at this stage, as the available external tracers and mass spectral characteristics do not provide sufficient evidence to robustly constrain its origin. Based on its temporal behaviour and compositional features, LO-OOA3 is more appropriately interpreted as a regional background OOA component. In response to the combined comments from the Editor and Reviewer #1, we have revised the related discussion in Section 3.2 (Page 12, L349 – L362) accordingly.

The diurnal profile of LO-OOA3 showed a clear nocturnal enhancement, with concentrations increasing after approximately 20:00 and reaching a maximum between 06:00 and 08:00. This accumulation is consistent with shallow nocturnal boundary layer conditions and limited vertical mixing, which favour the build-up of regionally transported and aged background OOA. The moderate positive correlation with RH (r = 0.45) further suggests that humid conditions may have facilitated its partitioning or accumulation. During daytime, LO-OOA3 concentrations declined and exhibited strong inverse correlations with photochemically related OVOCs (e.g., MVK+MACR, r = −0.69). The growth of the PBL after sunrise likely enhanced vertical mixing and dilution, further contributing to the daytime decrease. Together, these observations suggest that LO-OOA3 accumulated under stable nocturnal conditions and was progressively diluted and/or transformed during daytime photochemical aging. In terms of MS characteristics, LO-OOA3 exhibited the highest N:C ratio among the identified OOA factors. The dominant nitrogen-containing fragments were CHN^+ (m/z 27.01) and CH_4N^+ (m/z 30.03), together accounting for approximately 6% of the total LO-OOA3 signal. However, its weak correlation with pON (r = 0.06) suggests that the elevated N:C ratio did not correspond to a major contribution to pON variability. Overall, these features are consistent with LO-OOA3 representing a relatively less-oxidized regional background OOA component containing embedded nitrogen functionality.

- LO-OOA3 factor has relatively good negative correlation with biogenic tracers but its correlation with

RH or Chl are not high to suggest any real relationship. I think the explanation of this factor needs to be revised. Also, the concentration of this factor goes up at night and that's when, regardless of air mass origin, RH is higher, so there may not be necessarily a marine source for this factor.

We have revised the discussions here. Please refer to our previous response for the revised discussions.

- L376-377: incomplete sentence

We have revised the sentence here.

The higher OA production rate relative to the average PM_1 production rate, together with the absence of significant increases in other aerosol components (SO_4, organic and inorganic NO_3; Figure 7d–f), indicates that photochemical OA formation played a dominant role in the observed increase in total PM_1 mass after approximately 24 hours of $t_{\mathrm{anthrop-photo}}$.

- L388: it's important to highlight again the with O/C of LO-OOA being less than that of the background aerosols, any significant addition of LO-OOA would lower the overall O/C and hence mask the increase with aging that is expected. Note: L390-397 is duplicating the paragraph above.

Combine both the Editor and Reviewer #1's comments, we have revised the discussions in Section 3.3 (Page 13, L395 – L407):

However, there was a slight increase in the average bulk O:C ratio as a function of $t_{\mathrm{anthrop-photo}}$ only during the NW period. Indeed, the average bulk O:C ratio did not show a corresponding increase with $t_{\mathrm{anthrop-photo}}$ during the SW and NE period; instead, a slight decrease was observed at higher $t_{\mathrm{anthrop-photo}}$ during the NE period. The average bulk O:C ratio at $t_{\mathrm{anthrop-photo}} = 0$ was approximately 0.55 across all periods, which was higher than the O:C ratios of most LO-OOA factors (LO-OOA1–3). This suggests that the regional background OA was already substantially oxidized prior to further photochemical processing. Consequently, additional aging may not necessarily lead to large increases in the average bulk O:C ratio. Other field studies in remote areas also report oxidation indicators reached a steady state rather than continuing to rise with photochemical age (Irei et al., 2015). During the NE period, the temporal evolution of bulk O:C exhibited a non-monotonic behavior. Between 0 and 8 hours of $t_{\mathrm{anthrop-photo}}$, the increase in MO-OOA contributed to a rise in average bulk O:C ratio. However, after ~8 hours, the more rapid formation of LO-OOA1 led to a greater relative contribution of less-oxidized components, thereby lowering the overall bulk oxidation level. As a result, the average bulk O:C decreased as $t_{\mathrm{anthrop-photo}}$ increased from 8 to 20 hours. Measurements in American urban environments report that LO-OOA increase more rapidly than MO-OOA during periods of active photochemical processing (Guo et al., 2024; Rogers et al., 2025).

- What is the source of pON? Please include references where these species have been associated with

primary emissions.

We have added the description in the Introduction section (Page 2, L67–70)

Particulate Organic Nitrate (pON), an important part of OA formed either through primary emissions such as combustion-related sources (e.g. Reyes-Villegas et al. (2018)), or through the oxidation of VOCs in the presence of nitrogen oxide radicals and atmospheric oxidants (e.g. Ng et al. (2017)).

- Fig 8g: due to reactivity, toluene and benzene should decrease more than CO (which is reduced mainly due to dilution) with photochemical aging, so why isn't this trend obvious here except maybe slightly for the NE corridor.

We appreciate the Editor's concern. As noted in our earlier response, there are two reasons to lead this: a fraction of the m/z 93 signal was influenced by the fragmentation of monoterpenes, and biogenic emissions also contribute to benzenoid compounds. During the NE air mass dominated period, pollution levels were higher, resulting in higher anthropogenic emitted toluene concentrations, and therefore the decreasing trend of (toluene + benzene)/CO was more clearly observed compared to other periods. As toluene may not serve as a reliable tracer of anthropogenic primary sources here, we have moved the PTR-MS results to the SI. The discussion has been added to SI as Section S7 (Page 10, L81 – L105) to avoid further misunderstanding.

S7 Evolution of gas phase compounds due to photochemical aging

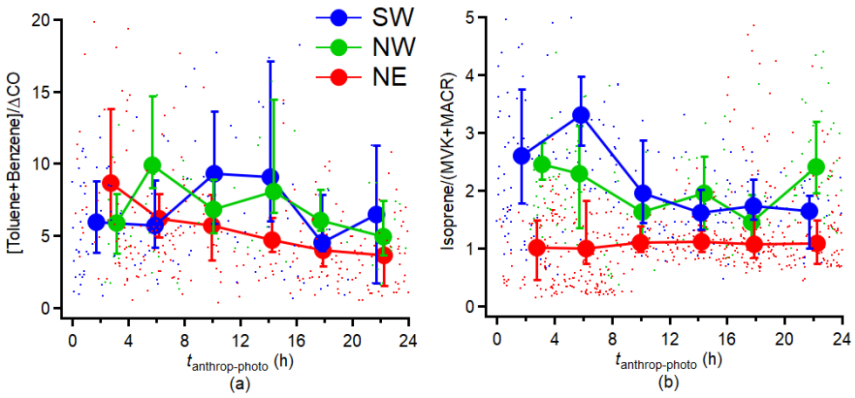

Figure S11: Variations in (a) the sum of toluene and benzene normalized to ΔCO concentration; (b) ratio between isoprene and MVK+MACR as a function of $t_{anthrop-photo}$. The results are averaged into four-hour intervals along $t_{anthrop-photo}$ and the error bar indicates the 25th and 75th percentiles, respectively.

Figure S11 presents the evolution of (a) sum of normalised toluene and benzene concentration. (b) ratio between isoprene and MVK+MACR as a function of $t_{anthrop-photo}$ The background CO was defined

as the 5th percentile of the entire campaign period (with BB influenced period removed) and was estimated to be 52 ppb. A decreasing trend was observed for the primary anthropogenic VOCs (Toluene + Benzene) during the NE period. However, the (Toluene + Benzene)/ΔCO concentrations remained independent of $t_{\mathrm{anthrop-photo}}$ for the other periods. This was likely attributable to either instrumental interference, as a fraction of monoterpenes is known to fragment under PTR-MS ionization conditions, producing ions at m/z 93 (Tani et al., 2003; Ambrose et al., 2010), or to biogenic emissions of toluene from certain plant species (Misztal et al., 2015; White et al., 2009). During the NE air mass dominated period, pollution levels were higher, resulting in higher anthropogenic emitted toluene concentrations. Under these polluted conditions, the relative contribution of interference from biogenic emissions became less significant, and the decreasing trend of (Toluene + Benzene)/ΔCO was more clearly observed compared to other periods.

As shown in Figure S11(b), the ratio of isoprene to MVK+MACR decreased during the SW period, while its variation was limited during the NE period. This was likely due to both enhanced daytime isoprene emissions and more active photochemical process of MVK+MACR under the strong solar radiation and high temperatures characteristic of the NE period.

- FigS10: what's the interpretation of much stronger deviation for LO-OOA2 between above/below canopy measurements? I think this helps explaining the source of LO-OOA2 and a discussion on this should be added to the main text.

We thank the editor for the comments. A decoupling of O_3 concentrations between the above- and below-canopy layers was observed at night during the experimental period, as presented in Dewald et al. (2024), who reported that nighttime monoterpene oxidation was primarily driven by O_3 chemistry. This oxidation led to enhanced O_3 consumption below the canopy, resulting in lower O_3 concentrations compared to the above-canopy layer. Combined Reviewer #1's comments we have revised the discussions in Section 3.2 (Page 11, L332 – L340):

LO-OOA2 exhibited a pronounced nocturnal maximum and showed the strongest correlation with monoterpenes among the measured VOCs, indicating a close link to monoterpene oxidation. As shown in Figure S10, LO-OOA2 concentrations were decoupled between the above- and below-canopy layers at night, with enhanced levels observed below the canopy. This vertical gradient suggests that LO-OOA2 formation was strongly influenced by locally emitted monoterpenes from surrounding vegetation. Dewald et al. (2024) reported that nighttime monoterpene oxidation was predominantly driven by O_3 during the experimental period. Under shallow nocturnal boundary layer conditions, vertical mixing of O_3 between the above- and below-canopy layers was suppressed. As a result, enhanced monoterpene oxidation below the canopy caused more rapid O_3 depletion relative to the above-canopy layer at night.

- Table S3. What are the uncertainties in the fitted parameters representing? Was variability in the data

used in any way to constrain the fitted parameters?

In the original manuscript, the exponential fitting was performed using an ordinary (unweighted) nonlinear least-squares approach applied to four-hour bin averaged data in order to enhance the signal-to-noise ratio. No additional weighting or variability-based constraints were imposed.

Following the suggestion of Reviewer #2, we have revised the analysis to use absolute concentrations. Although the overall trends and conclusions remain unchanged, the statistical robustness of the exponential fit becomes less pronounced. We have therefore removed the fitting analysis from the revised manuscript. This modification does not affect the main findings or final conclusions of the study.

- Since there were many occasions of wildfires in the region, are there any tracers from PTR-MS that can be used to track the influence of BB plumes in the data? (e.g. acetonitrile)

We appreciate the editor's suggestions. The variation of acetonitrile was limited during the whole measurement period except on 19 July. In addition, molecular analysis using a high-resolution mass spectrometer (HR-MS) was conducted to identify the tracers from the potential emission sources, and the results are reported in a separate study from the same campaign period. That study identified a significant increase in the BB tracer nitrocatechols ($C_6H_5NO_4$) only on 19th July during the ACROSS campaign, while its relative intensity remained below 2% for the rest of the campaign (Pereira et al., 2025). These results indicate that the influence of BB emissions at the measurement site was limited throughout the campaign, except on 19 July. We have revised the related discussion in Section 3.1 (Page 9 – Page 10, L279 – L283), and we also fixed the typo here regarding to the BB event date:

Pronounced increases in PM_1 mass concentration and acetonitrile were observed on the evening of 19 July during periods dominated by SW and SE air masses, indicating a BB event. However, acetonitrile concentrations exhibited only limited variability during the rest of the measurement period. In addition, molecular analysis over the campaign period identified a significant enhancement of the BB tracer (nitrocatechols, $C_6H_5NO_4$) only on 19 July (Pereira et al., 2025). These results indicate that BB emissions made a limited contribution during the campaign, apart from the event on 19 July.

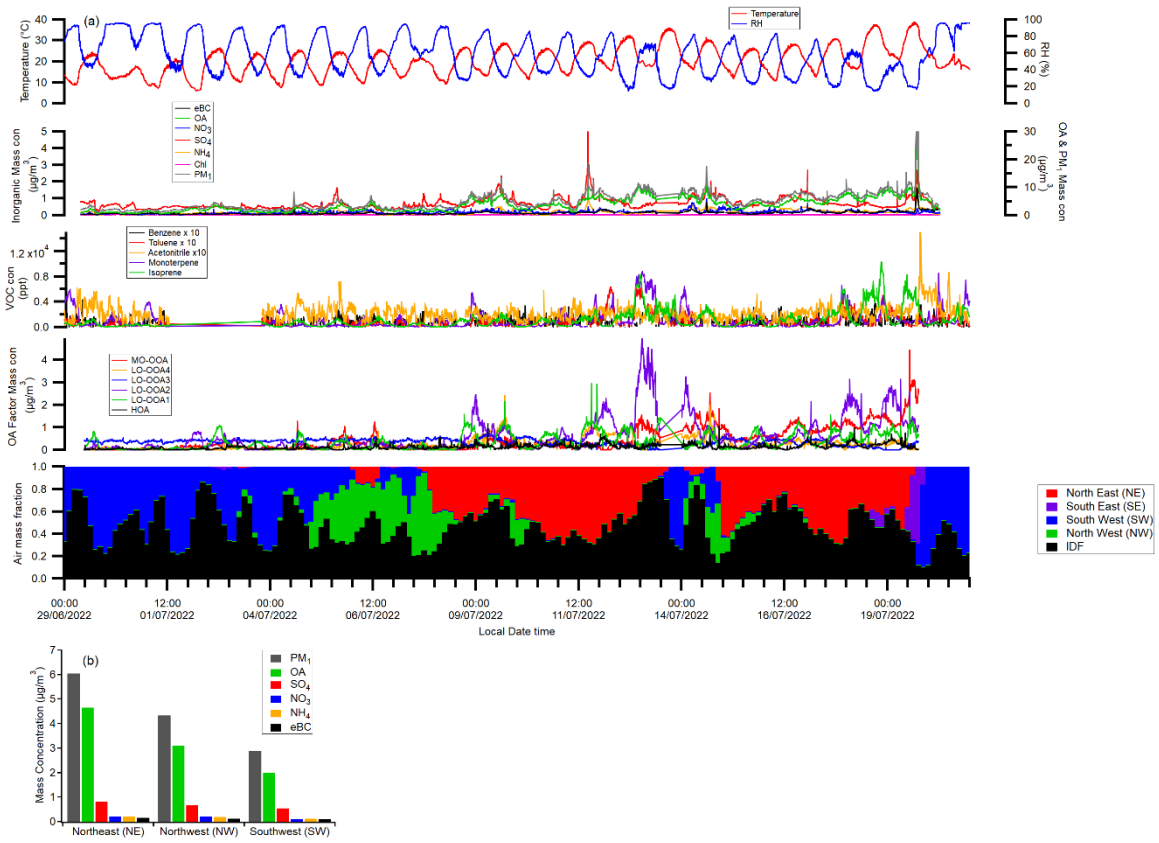

Reviewer#1

In their revised manuscript, all of my (Reviewer#1) previously raised specific comments and technical corrections were addressed. The authors justified the main concern of using ground observation below-canopy to characterize aerosol properties influenced by regional transport, providing evidence that localized plumes had only a minor effect under a well-mixed canopy condition during the daytime. The added information solidified the methodology and enabled the subsequent evaluation of the results and conclusions, which is the focus of this review.

Specific comments:

1. I have concerns in the conclusion that rapid formation of MO-OOA contributed to the BrC increase during the daytime. We know from your introduction that 1) nitrogenous OA can contribute to the light absorption by BrC during aging, and 2) the bleaching of BrC through intense photooxidation processes is widely observed. In your results, for the strong solar radiation scenario, were you able to see any diurnal pattern of BrC vs. O:C ratio and f44? Did the absorption keep climbing with f44 throughout the day, or did they decouple later in the day? If your "MO-OOA" factor had high N/C or strong nitrate-related fragments, it might really be a secondary BrC factor that happened to be categorized into MO-OOA. I am not entirely confident with the generic conclusion that "the rapid formation of MO-OOA contributed to the BrC increase during the daytime" without having the above concerns

reviewed/addressed.

In addition, I also did not see any description of BrC mass change under humid, low-radiation conditions as the contrast group. Note that your LO-OOA3 has the highest N/C among your factors. Yet your daytime photochemical indicators seemed to have a negative influence on it (e.g. Line 330-ish). Is there any discussion that could be expanded on this point? Why did LO-OOA3 get "effectively degraded" while MO-OOA were "rapidly forming"? Are the oxidants really capable of distinguishing and treating them differently in the physical world? Have you considered the possibility that the formation of your N-rich MO-OOA is actually an oxidation/conversion from your N-rich LO-OOA3?

We appreciate the reviewer's concern. In response to the reviewer's question regarding diurnal variations under strong solar radiation conditions, we present the diurnal profiles of the BrC absorption coefficient at 470 nm and the bulk average O:C ratio during the NE period in the response. The BrC absorption coefficient increased with the bulk average O:C during the daytime. The BrC absorption coefficient decreased later after. As the bulk average O:C ratio was higher than those of most LO-OOA components, the observed increase in the mid of the day likely reflected an enhanced contribution from MO-OOA. In the later afternoon, however, the bulk O:C ratio declined, likely due to the increasing contribution of LO-OOA1, which was with a much lower O:C ratio and consequently reduced the bulk-averaged oxidation level but the LO-OOA1 has limited impact on BrC.

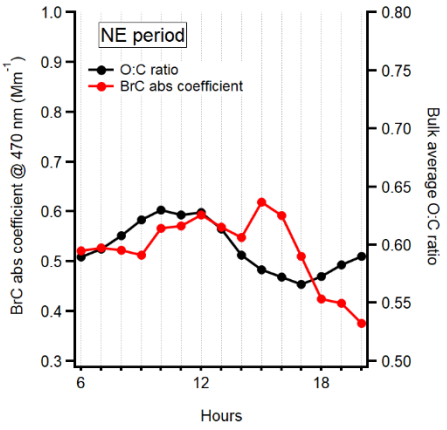

This co-variation of bulk average O:C ratio and BrC absorption coefficient suggests that a portion of BrC may be associated with MO-OOA. While partial photochemical bleaching cannot be excluded during photochemical process, our results did not indicate that bleaching was the dominant process during photochemical aging in the present observations. Instead, MO-OOA likely retained an overall light-absorbing character during the campaign. We agree with the reviewer that a potential pathway may exist whereby "N-rich MO-OOA represents oxidation or transformation from N-rich LO-OOA3". However, this interpretation cannot be conclusively verified. MO-OOA likely represents a more oxidized composite mixture derived from multiple precursor sources and oxidative pathways, and thus it does not consistently retain high N:C ratios or strong nitrate-related signatures.

We have revised the discussion related to the correlation between BrC absorption and PMF-derived factors. We have also updated Table 1 to report the multivariate correlation coefficients instead of the simple bivariate correlation coefficients for clarity:

$\sigma_{\text{abs BrC,470}}$ ($R^2 = 0.54$)		
HR-AMS PMF factor	Regression coefficient a_i	Partial correlation coefficient (multivariate)
HOA	0.47	0.22
LO-OOA1	-	-
LO-OOA2	0.04	0.09
LO-OOA3	0.57	0.25
LO-OOA4	0.30	0.30
MO-OOA	0.40	0.59
Intercept		-0.13

Table 1. Results of multiple linear regression (MLR) between $\sigma_{\text{abs BrC,470}}$ and individual PMF-derived factors. The final regression excludes the LO-OOA1 due to its negative regression coefficient value (-0.06). The Variance Inflation Factors (VIF) for HOA, LO-OOA2, LO-OOA3, LO-OOA4, and MO-OOA were 1.48, 1.16, 1.71, 2.27 and 1.31, respectively. Results include all the PMF-derived factors are presented in Table S2 in the supplementary.

We have revised the discussion in Section 3.5 (Page 15 – Page 16, L465 – L478):

Table 1 presents the results of the regression factors of the MLR analysis between $\sigma_{\text{abs BrC,470}}$ and PMF-derived factors. The multivariate correlation coefficient is also presented to illustrate the contribution of each PMF-derived factor to the total BrC absorption during the whole experiment period. Interestingly, the LO-OOA3 and MO-OOA, which have the highest nitrogen content among all factors, also depict high MAC (regression coefficients). However, their multivariate associations with BrC differed substantially. MO-OOA showed the highest partial correlation with BrC among all the factors. In contrast, although LO-OOA3 displayed a relatively high MAC, its partial correlation with BrC was limited, suggesting a weaker contribution to the overall increase of BrC absorption during the daytime. One possible explanation is that LO-OOA3 represented a relatively labile nitrogen-containing precursor pool that underwent further transformation during daytime photochemical processing, with part of its chromophoric contribution being transferred to the more oxidized MO-OOA component. While this scenario is possible, it cannot be explicitly confirmed due to MO-OOA comprised contributions from multiple sources and oxidation pathways. Although bleaching of BrC after intensive photooxidation was observed in previous studies (Zhao et al., 2015), our results did not indicate that bleaching was the dominant process during photochemical aging in the present observations. Under the oxidative conditions encountered here, MO-OOA likely retained net light-absorbing properties and continued to contribute to BrC absorption.

We have added descriptions about the SW period in Page 15, L453-456:

As $t_{\mathrm{anthrop-photo}}$ increased from around 2 hours to nearly 24 hours, the average BrC absorption fraction rose from about 17% to 23% in the NE period and from roughly 18% to 26% in the NW period. For the SW period, the average BrC absorption fraction remained relatively constant during the first 20 hours of $t_{\mathrm{anthrop-photo}}$ and increased to approximately 25% after 24 hours of $t_{\mathrm{anthrop-photo}}$.

Also in the following discussions in Page 16, L486-492:

Combined with the photochemical aging process discussed in Section 3.3, the decline in HOA concentration with photochemical aging during the NE and NW period demonstrated a reduced contribution of primary BrC following a relative ~24-hour photochemical aging process. In contrast, the BrC absorption fraction increased with $t_{\mathrm{anthrop-photo}}$, consistent with enhanced formation of secondary BrC. The covariance between MO-OOA and the BrC absorption fraction suggests that MO-OOA formation was associated with increased short-wavelength BrC absorption, especially under high solar radiation conditions during the NE and NW periods. By comparison, during the SW period, MO-OOA formation was less pronounced, and the corresponding increase in BrC absorption fraction with photochemical aging was also limited.

We acknowledge that the original conclusion may not have been sufficiently precise, and we agree that the use of the term "rapid" was not justified in this context. The observed covariance between MO-OOA and BrC indicates a clear association between the two; however, this relationship should not be interpreted as a direct mechanistic contribution. We have revised the Abstract and Conclusion sections accordingly.

Abstract section (Page 1, L33-36) as:

Meteorological conditions played a critical role: under dry and strong solar radiation conditions, enhanced formation of more-oxidized OOA (MO-OOA) was observed. BrC absorption increased concurrently, with short-wavelength absorption rising by ~35% over relatively ~24 hours of photochemical aging.

Conclusion section (Page 17, L518-522) as:

By contrast, under dry, high-radiation conditions, enhanced photochemical processing was associated with increased formation of MO-OOA. During these periods, primary anthropogenic OA and nitrogen-enriched LO-OOA decreased, while MO-OOA increased concurrently. The contribution of short-wavelength BrC absorption increased with relative anthropogenic photochemical age and coincided with enhanced MO-OOA formation.

2. Around Line 305, I suggest toning down the "explanation" of nighttime peak of LO-OOA2 to monoterpene-SOA to more of an "implication" without quantitative evidence from PBL, nighttime O3, OH, and nitrate radical data integration. Something like "The factor exhibits a nocturnal maximum and

correlates best with monoterpenes among measured VOCs, implying a strong contribution from monoterpene-derived biogenic SOA, likely enhanced at night by a shallow boundary layer, lower temperatures, and NO3-initiated oxidation." In my opinion, that very low N:C of LO-OOA2 makes "classic NO3-initiated monoterpene-SOA" unlikely as the dominant component of your factor. If you'd like to dig deeper, does the NO^+/NO_2^+ ratio co-vary with the factor? Does the factor ever show higher N:C in periods with high NOx and O3 at night? It might not be a focus of your current study but rather an interesting point to look into for your in-preparation nighttime above- and below-canopy differences work.

We agree with the reviewer that the low N:C ratio of LO-OOA2 makes it unlikely to represent NO_3-initiated monoterpene SOA. Instead, a difference in O_3 concentrations between above- and below-canopy measurements during nighttime, which may provide additional insight into its formation. We have revised the related discussion accordingly, please refer to our response to the Editor's comments for details. However, a comprehensive discussion of the nighttime formation mechanisms of LO-OOA2 may beyond the scope of the present study, as our focus is on the physicochemical properties of aerosols during the daytime. We thank the reviewer for this valuable suggestion, which will be considered in our future work.

3. Around Line 315, same issue as above, your LO-OOA3 diurnal trend is so gentle that could totally be due to the change in PBL. If PBL data are available, it is recommended that you normalize your diurnal profiles of OA factors by it. I also do not think r = 0.45 and 0.4 (not r-square) can suggest anything. Your chloride is so low that I guess for the majority of your campaign period, it might be below the detection limit (yours, not DeCarlo's). Please add a column to Table S1 to report the average +/- std of your five main AMS species. They are hard to be perceived from Figure 2. As a result, I do not really consider the subsequent discussions about sea-salt chloride etc are valid and necessary. Please clarify or revise accordingly.

We have revised the discussion of LO-OOA3 accordingly. Although direct PBL measurements were not available during this campaign, we agree with the reviewer that the daytime growth of the PBL likely contributed to the observed decrease in LO-OOA3 concentrations. Please refer to our response to the Editor's comment for the revised discussion. In addition, the AMS detection limits have been added in Table S1. Please refer to our response to Minor comment 4 for the revised table.

4. Starting from Line 380 to 397, I am unsure of the logic behind a decreased O:C during the NE due to additional LO-OOA formation. If what you explained here was true, then the new formation of LO-OOA needs to outpace the aging of MO-OOA, in order to "dilute the overall oxidation level and lower the average bulk O:C ratio." It is contradictory to your other results, e.g. the rapid formation of MO-OOA during the NE period, and is not backed by Figure S11 (magnitude of MO-OOA increase > LO-OOA1 increase, and LO-OOA2 to 4 changed negligibly). However, if you'd like to have more recent supportive evidence for your OOA formation from photochemical processes in urban areas, you could refer to

-Guo et al., 2024 (https://doi.org/10.1016/j.atmosenv.2024.120362) in San Antonio

-Rogers et al., 2025 (https://doi.org/10.1029/2024GL112005) in New York City

They observed the positive influences of photochemistry on OOA mass with AMS/ACSM-PMF in the 7th and 1st largest cities in the U.S.

We appreciate the reviewer's concern; however, the results are not contradictory. As shown in Figure S11(f), during the NE period, MO-OOA increased rapidly within the first 8 hours of $t_{\text{anthrop-photo}}$, which led to an increase in the average bulk O:C ratio over this initial period. After approximately 8 hours of $t_{\text{anthrop-photo}}$, MO-OOA showed less further increase until ~20 hours of $t_{\text{anthrop-photo}}$. In contrast, as shown in Figure S11(b), LO-OOA1 increased more substantially after 8 hours of $t_{\text{anthrop-photo}}$,. The enhanced contribution of LO-OOA1, which has a much lower O:C ratio (O:C = 0.29), reduced the bulk average O:C ratio. This shift in relative contributions explains the slight decrease in bulk O:C observed when $t_{\text{anthrop-photo}}$ exceeded 8 hours during the NE period. In response to the reviewer's comment, we have included the diurnal variations of the bulk average O:C ratio as well as MO-OOA and LO-OOA1 mass concentrations between 6:00 and 20:00. The results show that in the late afternoon, when LO-OOA1 concentrations exceeded those of MO-OOA, the bulk average O:C ratio declined. The revised discussions are presented in our response to Editor's comments. We have also included the suggested references in the discussions.

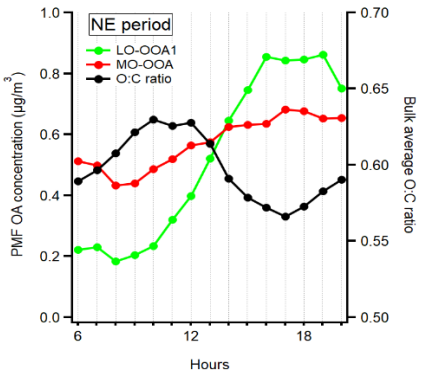

5. I suggest avoiding putting "emissions" to any SOA (e.g. "near-ground emissions of LO-OOA2 from local vegetation"), simply because any SOA by definition is secondary, not directly emitted from a specific source. It is a minor thing but really reads counterintuitive. Sanity checks over both the manuscript and SI would be appreciated.

Accept, we have revised the relevant sections of the manuscript and SI accordingly. We have revised the wording by replacing "emission" with "formation".

Technical corrections:

1. Line 68, "...formed in the oxidation of VOCs in the…"

Accept. The revised text is provided in our response to the Editor's comments.

2. Line 83, "...previous AMS-PMF analysis during…"

Accept.

Previous AMS-PMF analysis during summertime have shown that

3. SI, Line 69, "...observed at night till the early dawn…"

Accept.

Throughout the campaign, differences in NR-PM_1 between the two heights were only observed at night till the early dawn the next day.

4. SI, Table S1, detection limits of your specific HR-AMS should be calculated from your in situ filtered periods not adopted from DeCarlo et al. (2006). According to your response, filtered periods were performed periodically daily. You can either lump them together for a set of campaign-average MDLs or estimating MDLs for individual periods at the beginning, middle, and the end of your campaign and report a set of averages.

Accept. We have revised Table S1:

IE	3.00E-07	
	RIE	Detection limit of HR-AMS V-mode (μg/m³)
OA	1.4	0.069
SO4	0.88	0.022
NO3	1.1	0.016
NH4	4	0.070
Chl	1.3	0.022

Table S1: Ionization Efficiency (IE) and Relative Ionization Efficiency (RIE) applied for HR-AMS data analysis. Detection limits for NR-PM_1 species were calculated as three times the standard deviation (3σ) of mass concentrations measured during filter periods, following the approach of Decarlo et al. (2006). The HR-AMS data were recorded at a ~3 min time resolution.

5. Section 3.2, Line 282-290, multiple Figure numbering in this paragraph is inaccurate.

Accept.

Figure 4 presented the average mass spectra of the resolved six PMF OA factors: one Hydrocarbon-like OA (HOA) and five OOA factors. The Pearson correlation coefficient (r) between the HR-AMS PMF factors and the external tracers is presented in Figure 5. The time series of the PMF-derived OA factors between June 29 and July 20, 2022, is presented in Figure 2(a). Figure 3(i) shows the diurnal variations of the OA factors, and Figure 6 presents the mass fractions of the OA factors according to the dominated air mass periods.

6. Figure 6, please consider adding mass concentration next to each percentage given the total OA mass of each pie is different.

Accept. However, presenting the concentrations of all OA factors next to their percentage would compromise the readability of the figure. Therefore, we have added the average OA mass concentration for each period instead.

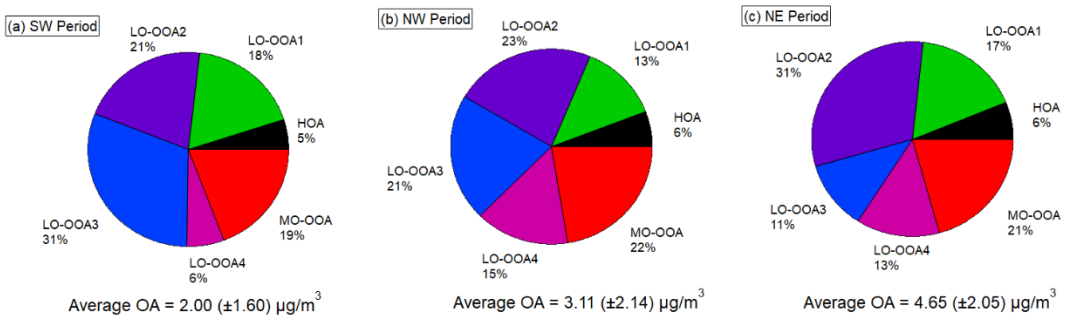

Figure 6: Pie charts for the mass fractions of different PMF OA factors during the three different airmass dominated periods. Values are reported as mean ± standard deviation.

7. Line 321, I guess you're referring to Table S2?

Accept, we have revised the discussions here. The revised discussions related to LO-OOA3 is presented in our response to Editor's comments.

8. Line 341, "The MO-OOA…"

Accept, we have fixed the typo here:

The MO-OOA was with the highest average O:C ratio (0.86) among all the factors, and dominant peaks were presented at m/z 28 (CO+) and 44 (CO2+).

Reviewer#2

Major Comment 1 (photochemical age):

A major limitation of the current methodology is that the photochemical age inferred from NOx/NOy is not well suited for a ground-based site where air masses change continuously. This approach is appropriate in studies such as Kleinman et al. (2007), Parrish et al. (2007), and Nault et al. (2018), which rely on aircraft measurements that more closely follow evolving air parcels. Hayes et al. (2013) applied a ground-based approach but explicitly evaluated the errors introduced when an air parcel continues to receive fresh emissions during transport to the measurement site.

In the present study, although the authors state that the sampled air is clean and well mixed, this does not resolve the core issue that the measurements do not track the same air parcel from emission to downwind. Reframing the metric as "relative anthropogenic photochemical age" does not address this limitation and instead obscures the importance of mixed anthropogenic and biogenic influences emphasized in the Introduction.

We respectfully disagree with the reviewer's comments here.

Firstly, while we acknowledge that air masses evolve continuously in reality, our analysis was conducted within defined air mass dominated periods identified based on transport origin. Within each of these periods, the air masses exhibited relatively consistent characteristics in terms of source region and meteorological conditions. We have clarified this point in our previous response.

Secondly, we addressed the reviewers' concerns by incorporating an above-canopy analysis in our previous revised manuscript, which demonstrates that the boundary layer was well mixed during the daytime throughout the campaign period. The influence of localized emissions and nearby plumes during daytime was minimal and does not compromise the conclusions of this study. As the measurement site (which is 50 km from Paris urban area) is situated outside the primary NO_x emission hotspots identified in regional inventories, this will support the estimation of photochemical age using NO_x/NO_y method.

Thirdly, following the Editor's suggestion, we calculated an air-mass transport age using dispersion model analysis to provide an independent validation of $t_{\mathrm{anthrop-photo}}$. The estimated transport ages from the identified anthropogenic emission regions during each air mass dominated period show good agreement with the temporal variability of $t_{\mathrm{anthrop-photo}}$. This consistency supports our interpretation, as air masses with longer transport times are expected to undergo more extensive cumulative photochemical processing. This agreement suggests that the temporal variability in NO_x/NO_y was primarily governed by cumulative transport and photochemical processing, rather than being dominated by intermittent NO_x injections locally. Please refer to our response at the beginning for the revised results and discussions. We have also revised the Introduction accordingly to avoid further misunderstanding.

Major Comment 2 (dilution correction):

If OA and BC originate from the same source, the OA/BC ratio can be used to account for dilution as air

parcels mix with cleaner background air. However, in the present study, the authors state that the sampled air masses are “enriched with anthropogenic primary carbonaceous aerosols,” yet OA is not necessarily co-emitted with BC and may include contributions from secondary and non-combustion sources. The use of the OA/BC ratio for dilution correction is therefore not well justified.

As suggested by the reviewer, we have removed eBC as a dilutor in Section 3.3 and 3.4 in the revised manuscript. We have revised Page 14 – Page 15, L421 – L448, accordingly; please refer to the revised manuscript for the updated discussion. The overall conclusions remain unchanged, as eBC concentrations exhibited minimal daytime variability at the measurement site and did not substantially influence the interpretation. However, the statistical robustness of the exponential fit becomes less pronounced We have therefore removed the fitting analysis from the revised manuscript. This modification does not affect the main findings or conclusions of the study.

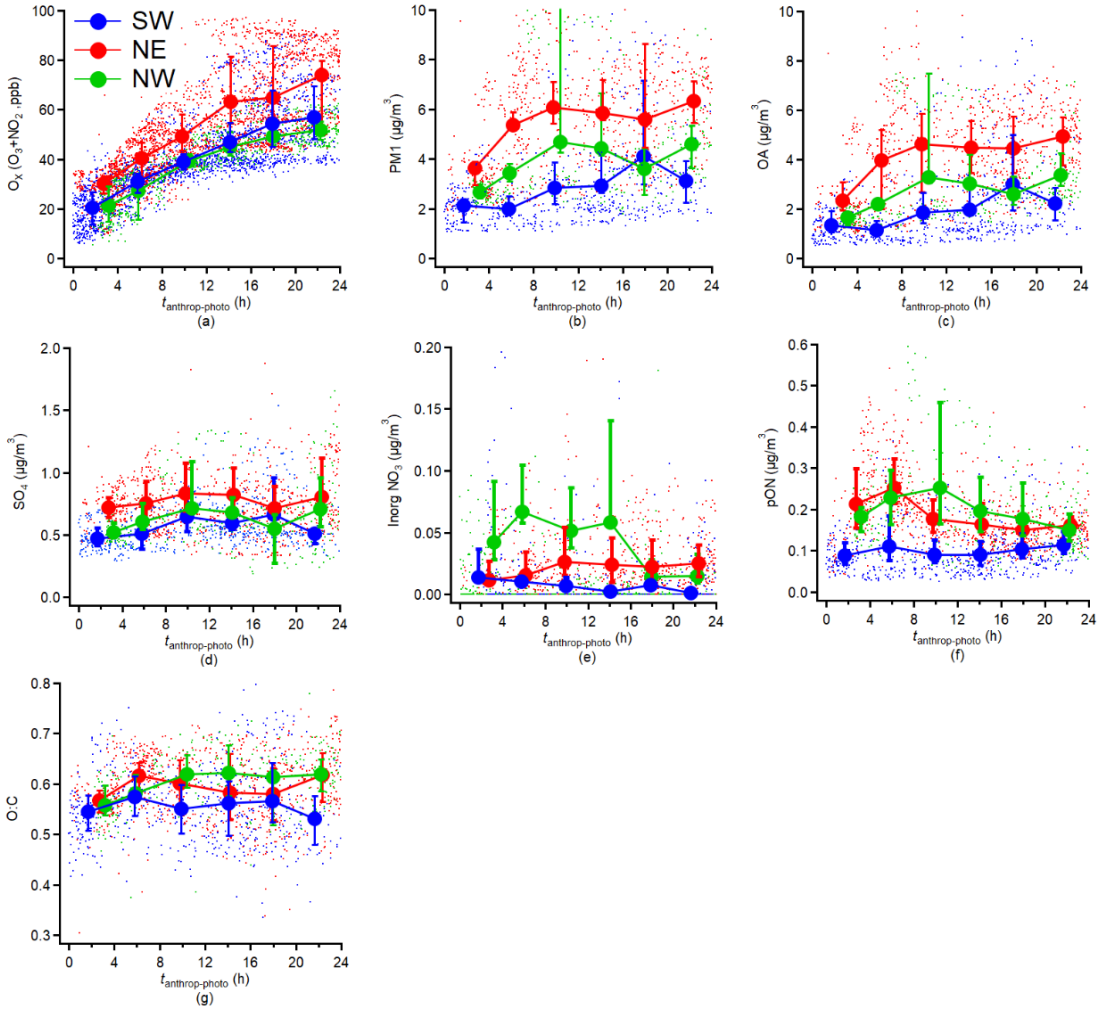

Figure 7: Variations in aerosol compositions concentrations: (a) O_x (O_3+NO_2) (b) PM_1 (c)OA (d) Sulfate (e) Inorganic nitrate (f) particulate Organic Nitrate (pON) (g) O:C ratio measured by HR-AMS as a function of $t_{anthrop-photo}$. The results are averaged into four-hour intervals along $t_{anthrop-photo}$ and the error bar indicates the 25th and 75th percentiles, respectively.

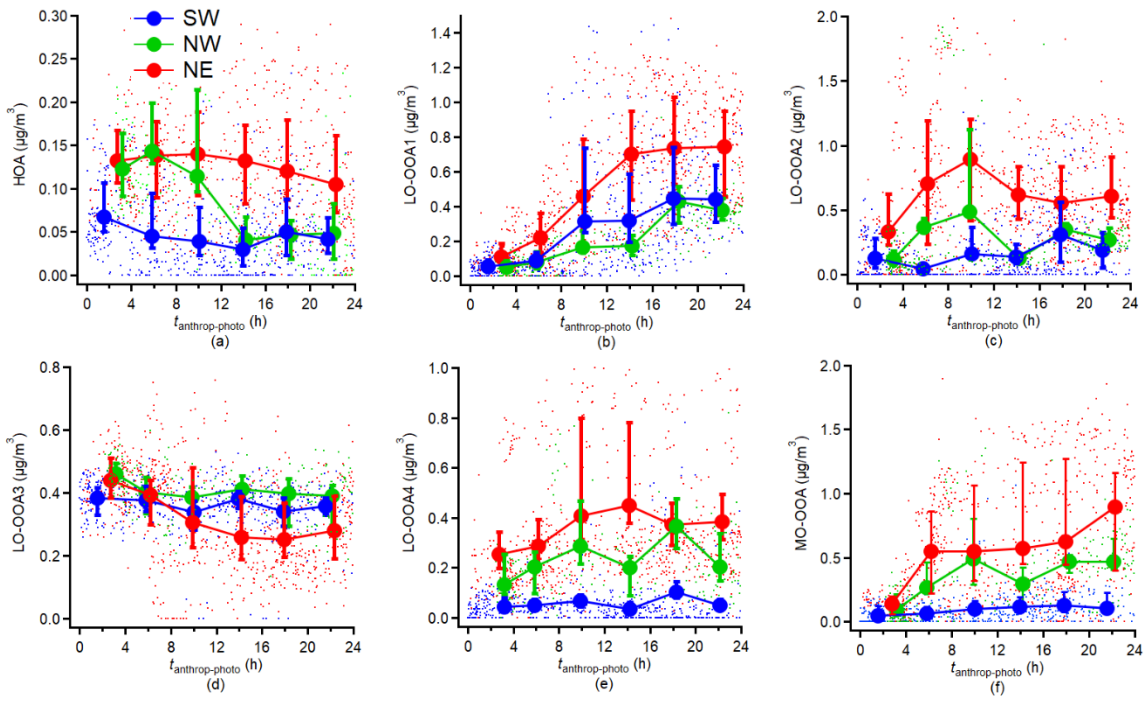

Figure 8: Variations in (a-f) HR-AMS PMF-derived factors normalised or non-normalised concentrations. The results are averaged into four-hour intervals along $t_{\mathrm{anthrop-photo}}$ and the error bar indicates the 25th and 75th percentiles, respectively.

References

Ambrose, J. L., Haase, K., Russo, R. S., Zhou, Y., White, M. L., Frinak, E. K., Jordan, C., Mayne, H. R., Talbot, R., and Sive, B. C.: A comparison of GC-FID and PTR-MS toluene measurements in ambient air under conditions of enhanced monoterpene loading, Atmos. Meas. Tech., 3, 959–980, 10.5194/amt-3-959-2010, 2010.

Crippa, M., Guizzardi, D., Pagani, F., Schiavina, M., Melchiorri, M., Pisoni, E., Graziosi, F., Muntean, M., Maes, J., Dijkstra, L., Van Damme, M., Clarisse, L., and Coheur, P.: Insights into the spatial distribution of global, national, and subnational greenhouse gas emissions in the Emissions Database for Global Atmospheric Research (EDGAR v8.0), Earth Syst. Sci. Data, 16, 2811–2830, 10.5194/essd-16-2811-2024, 2024.

DeCarlo, P. F., Kimmel, J. R., Trimborn, A., Northway, M. J., Jayne, J. T., Aiken, A. C., Gonin, M., Fuhrer, K., Horvath, T., Docherty, K. S., Worsnop, D. R., and Jimenez, J. L.: Field-Deployable, High-Resolution, Time-of-Flight Aerosol Mass Spectrometer, Analytical Chemistry, 78, 8281–8289, 10.1021/ac061249n, 2006.

Dewald, P., Seubert, T., Andersen, S. T., Türk, G. N. T. E., Schuladen, J., McGillen, M. R., Denjean, C., Etienne, J. C., Garrouste, O., Jamar, M., Harb, S., Cirtog, M., Michoud, V., Cazaunau, M., Bergé, A., Cantrell, C., Dusanter, S., Picquet-Varrault, B., Kukui, A., Xue, C., Mellouki, A., Lelieveld, J., and Crowley, J. N.: NO3 reactivity during a summer period in a temperate forest below and above the canopy, Atmos. Chem. Phys., 24, 8983–8997, 10.5194/acp-24-8983-2024, 2024.

Guo, F., Bui, A. A. T., Schulze, B. C., Dai, Q., Yoon, S., Shrestha, S., Wallace, H. W., Sanchez, N. P., Alvarez, S., Erickson, M. H., Sheesley, R. J., Usenko, S., Flynn, J., and Griffin, R. J.: Airmass history, night-time particulate organonitrates, and meteorology impact urban SOA formation rate, Atmospheric

Environment, 322, 120362, https://doi.org/10.1016/j.atmosenv.2024.120362, 2024.
Misztal, P. K., Hewitt, C. N., Wildt, J., Blande, J. D., Eller, A. S. D., Fares, S., Gentner, D. R., Gilman, J. B., Graus, M., Greenberg, J., Guenther, A. B., Hansel, A., Harley, P., Huang, M., Jardine, K., Karl, T., Kaser, L., Keutsch, F. N., Kiendler-Scharr, A., Kleist, E., Lerner, B. M., Li, T., Mak, J., Nölscher, A. C., Schnitzhofer, R., Sinha, V., Thornton, B., Warneke, C., Wegener, F., Werner, C., Williams, J., Worton, D. R., Yassaa, N., and Goldstein, A. H.: Atmospheric benzenoid emissions from plants rival those from fossil fuels, Scientific Reports, 5, 12064, 10.1038/srep12064, 2015.
Ng, N. L., Brown, S. S., Archibald, A. T., Atlas, E., Cohen, R. C., Crowley, J. N., Day, D. A., Donahue, N. M., Fry, J. L., Fuchs, H., Griffin, R. J., Guzman, M. I., Herrmann, H., Hodzic, A., Iinuma, Y., Jimenez, J. L., Kiendler-Scharr, A., Lee, B. H., Luecken, D. J., Mao, J., McLaren, R., Mutzel, A., Osthoff, H. D., Ouyang, B., Picquet-Varrault, B., Platt, U., Pye, H. O. T., Rudich, Y., Schwantes, R. H., Shiraiwa, M., Stutz, J., Thornton, J. A., Tilgner, A., Williams, B. J., and Zaveri, R. A.: Nitrate radicals and biogenic volatile organic compounds: oxidation, mechanisms, and organic aerosol, Atmos. Chem. Phys., 17, 2103–2162, 10.5194/acp-17-2103-2017, 2017.
Pereira, D. L., Giorio, C., Gratien, A., Zherebker, A., Noyalet, G., Chevaillier, S., Alage, S., Almarj, E., Bergé, A., Bertin, T., Cazaunau, M., Coll, P., Di Antonio, L., Harb, S., Heuser, J., Gaimoz, C., Guillemant, O., Language, B., Lauret, O., Macias, C., Maisonneuve, F., Picquet-Varrault, B., Torres, R., Triquet, S., Zapf, P., Hawkins, L., Pronovost, D., Riley, S., Flaud, P. M., Perraudin, E., Pouyes, P., Villenave, E., Albinet, A., Favez, O., Aujay-Plouzeau, R., Michoud, V., Cantrell, C., Cirtog, M., Di Biagio, C., Doussin, J. F., and Formenti, P.: Molecular characterization of organic aerosols in urban and forested areas of Paris using high-resolution mass spectrometry, Atmos. Chem. Phys., 25, 4885–4905, 10.5194/acp-25-4885-2025, 2025.
Reyes-Villegas, E., Priestley, M., Ting, Y.-C., Haslett, S., Bannan, T., Le Breton, M., Williams, P. I., Bacak, A., Flynn, M. J., Coe, H., Percival, C., and Allan, J. D.: Simultaneous aerosol mass spectrometry and chemical ionisation mass spectrometry measurements during a biomass burning event in the UK: insights into nitrate chemistry, Atmospheric Chemistry and Physics, 18, 4093–4111, 10.5194/acp-18-4093-2018, 2018.
Rogers, M. J., Joo, T., Hass-Mitchell, T., Canagaratna, M. R., Campuzano-Jost, P., Sueper, D., Tran, M. N., Machesky, J. E., Roscioli, J. R., Jimenez, J. L., Krechmer, J. E., Lambe, A. T., Nault, B. A., and Gentner, D. R.: Humid Summers Promote Urban Aqueous-Phase Production of Oxygenated Organic Aerosol in the Northeastern United States, Geophysical Research Letters, 52, e2024GL112005, https://doi.org/10.1029/2024GL112005, 2025.
Tani, A., Hayward, S., and Hewitt, C. N.: Measurement of monoterpenes and related compounds by proton transfer reaction-mass spectrometry (PTR-MS), International Journal of Mass Spectrometry, 223-224, 561–578, https://doi.org/10.1016/S1387-3806(02)00880-1, 2003.
White, M. L., Russo, R. S., Zhou, Y., Ambrose, J. L., Haase, K., Frinak, E. K., Varner, R. K., Wingenter, O. W., Mao, H., Talbot, R., and Sive, B. C.: Are biogenic emissions a significant source of summertime atmospheric toluene in the rural Northeastern United States?, Atmos. Chem. Phys., 9, 81–92, 10.5194/acp-9-81-2009, 2009.
Zhao, R., Lee, A. K. Y., Huang, L., Li, X., Yang, F., and Abbatt, J. P. D.: Photochemical processing of aqueous atmospheric brown carbon, Atmos. Chem. Phys., 15, 6087–6100, 10.5194/acp-15-6087-2015, 2015.